

Quench Protection Studies for the High Luminosity LHC Nb₃Sn Quadrupole Magnets

Emmanuele Ravaoli ^{ID}, Giorgio Ambrosio ^{ID}, Member, IEEE, Hugues Bajas ^{ID}, Michal Duda, Paolo Ferracin ^{ID}, Jose Ferradas Troitino ^{ID}, Susana Izquierdo Bermudez ^{ID}, Franco Mangiarotti ^{ID}, Vittorio Marozzi ^{ID}, Matthias Mentink ^{ID}, Felix Rodriguez-Mateos, Ezio Todesco ^{ID}, Arjan P. Verweij ^{ID}, and Daniel Wollmann ^{ID}

Abstract—Achieving the targets of the High Luminosity LHC project requires the installation of new inner triplet magnet circuits for the final focusing of the particle beams on each side of the two main interaction points. Each of the four circuits will include six 150 mm aperture, 132.2 T/m gradient, Nb₃Sn quadrupole magnets to be installed in the LHC tunnel. The recently updated circuit topology is such that the protection of each magnet can be studied from a single magnet point-of-view. To limit the hot-spot temperature and the peak voltage-to-ground, a protection system was designed that quickly and reliably transfers voluminous parts of the coil to the normal-conducting state, hence distributing more homogeneously the magnets stored energy in the windings. This system is based on two elements: quench heaters attached to the outer layers of the magnet coils and CLIQ (Coupling-Loss Induced Quench). The performance of the protection system is investigated by simulating the electro-magnetic and thermal transients occurring after a quench with the program STEAM-LEDET, and by conducting dedicated experiments at the CERN and FNAL magnet test facilities. The effectiveness of the quench protection system is assessed at all representative operating current levels. Furthermore, the coils hot-spot temperature and peak voltage to ground are analyzed for various failure cases, conductor parameters, and parameter distribution among the four coils. It is concluded that the proposed design assures an effective, reliable, and fully redundant quench protection system.

Index Terms—Accelerator magnet, CLIQ, circuit modeling, quench protection, superconducting coil.

I. INTRODUCTION

INNER TRIPLET (IT) magnet circuits are required for the final focusing of the particle beams on each side of the two main interaction points of the Large Hadron Collider (LHC).

Manuscript received November 25, 2020; revised January 8, 2021; accepted January 21, 2021. Date of publication January 28, 2021; date of current version March 16, 2021. This work was supported in part by the U.S. Department of Energy, Office of Science, Office of High Energy Physics, through the U.S. LHC Accelerator Upgrade Project (AUP) and in part by the High Luminosity LHC Project at CERN. (*Corresponding author: E. Ravaoli.*)

Emmanuele Ravaoli, Hugues Bajas, Jose Ferradas Troitino, Susana Izquierdo Bermudez, Franco Mangiarotti, Matthias Mentink, Felix Rodriguez-Mateos, Ezio Todesco, Arjan P. Verweij, and Daniel Wollmann are with CERN, Geneva 1211, Switzerland (e-mail: Emmanuele.Ravaoli@cern.ch).

Michal Duda was with CERN, Geneva 1211, Switzerland. He is now with PSI, Villigen 5232, Switzerland.

Giorgio Ambrosio and Vittorio Marozzi are with the FNAL, Batavia, Illinois 60510-0500 USA.

Paolo Ferracin is with LBNL, Berkeley, CA 94720 USA.

Color versions of one or more figures in this article are available at <https://doi.org/10.1109/TASC.2021.3055160>.

Digital Object Identifier 10.1109/TASC.2021.3055160

For the LHC upgrade to High Luminosity [1]–[3], the existing circuits will be replaced with circuits featuring six 150 mm aperture, 132.2 T/m gradient, two-layer, Nb₃Sn quadrupole magnets (MQXF) [4]–[7]. These magnets, whose main parameters are listed in Table I, were jointly developed by CERN and the US LHC Accelerator Research Program (LARP) and HL-LHC Accelerator Upgrade Project (AUP), and are being manufactured in two versions with magnetic lengths of 4.2 m and 7.15 m [8].

In the case a small part of the superconducting coils of these high-field, high energy-density magnets suddenly becomes normal-conducting, a phenomenon known as quench, fast and non-uniform conductor heating and high internal coil voltages could pose a risk to the magnet integrity. An active system that detects the quench and transfers most of the coil winding pack to the normal state in a few tens of milliseconds is necessary in order to avoid damage due to overheating, which can cause permanent conductor degradation, or excessively high voltages to ground, which can damage the coil insulation layers. The quench protection of the IT circuit, which was studied in the recent years [10]–[12], is presented here for recently refined nominal and ultimate current levels [9], and updated circuit configuration. The updated IT circuit, shown in Fig. 1, includes parallel elements across each magnet, so that the protection of each magnet is independent from the others. Warm diodes are not required across Q1 magnets because the 35 A crowbar (CR) already provides an effective parallel path.

The magnet protection system includes two elements [10], [12], [13], namely quench heaters (QH) attached to the coils outer surface [14], [15], and the Coupling-Loss Induced Quench (CLIQ) system [16]–[18]. Each of the six magnets is protected by eight independent 900 V, 7.05 mF QH power supplies and one 40 mF CLIQ unit. CLIQ units protecting the 4.2 m and 7.15 m magnets are charged to 600 V and 1000 V, respectively. In the case a quench is detected in any of the magnets, the protection elements of all six magnets are triggered simultaneously.

The electro-magnetic and thermal transient following a quench was extensively studied by means of the STEAM-LEDET [19], [20] (Lumped-Element Dynamic Electro-Thermal) program, which was validated against experimental results collected while individually testing the 1.2 m and 4.0 m long model/prototype versions of the MQXF magnet [21]–[23].

The quench protection system performance is assessed at all foreseen operating current levels. Furthermore, the impact of

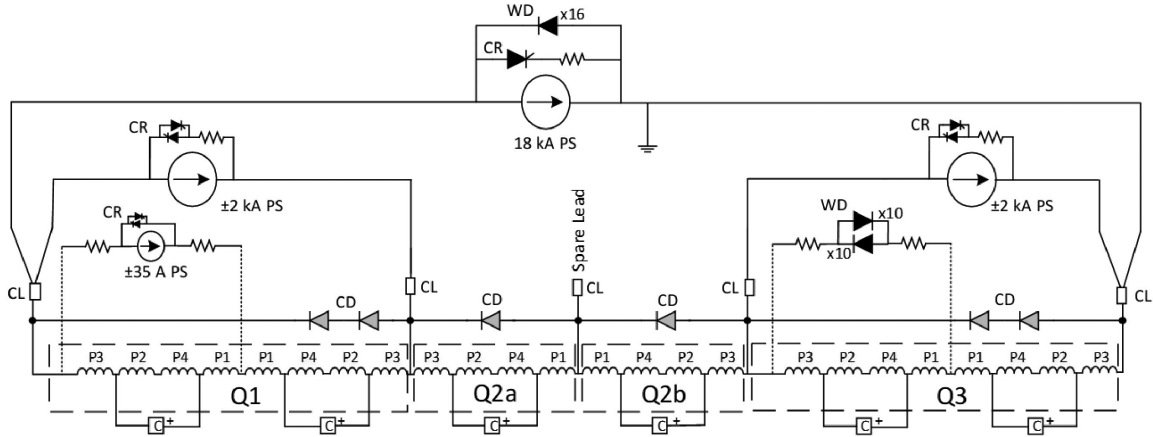


Fig. 1. Schematic of the powering and protection scheme of each Inner Triplet circuit including six Nb₃Sn quadrupole magnets assembled in four cold masses (Q1, Q2a, Q2b, Q3), one 18 kA power supply (PS), two ± 2 kA trim power supplies, one ± 35 A trim power supply, power-supply crowbars (CR), warm diodes (WD), cold diodes (CD), current leads (CL), and six CLIQ units (C). The four coils of each magnet are denoted with P1-P4. Pole P1 is the one located in the top right quadrant, viewing the magnet from the connection-side end; P2-P4 are numbered counter-clockwise.

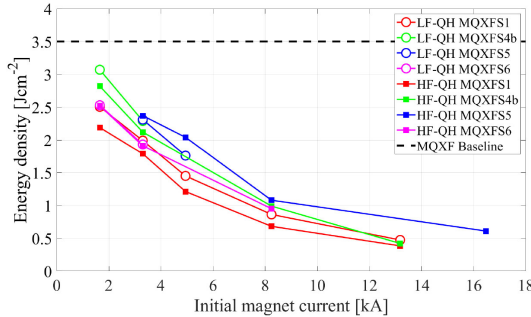


Fig. 2. Minimum QH energy density required to initiate a quench in the coil, measured on four MQXF short model magnets [14], [15], [24]–[27].

failure cases and conductor parameters on the coils hot-spot temperature and peak voltage to ground is investigated.

II. BASELINE QUENCH PROTECTION SYSTEM

The combined QH and CLIQ quench protection system is designed to assure safe circuit operation at any current level even in case of simultaneous failures of two protection units. In this study, the focus is on the 7.15 m magnet version. The hot-spot temperatures T_{hot} [K] of both versions are very similar, while their peak voltages to ground $U_{g,\text{peak}}$ [V] approximately scale with the magnet length.

The QH system is designed to initiate a resistive transition in the coil at currents as low as 1 kA. Each unit delivers a peak power density of about 220 W/cm² in the strip heating stations, decaying with a time constant of about 32 ms. Hence, the baseline deposited energy calculated adiabatically is about 3.5 J/cm². In order to evaluate the margin with respect to the minimum energy required to initiate a transition, dedicated tests were performed on multiple short model magnets [14], [15], [24]–[28]. The observed minimum energy density to quench, for a QH located at the low-field (LF-QH) and high-field (HF-QH) coil turns, is shown in Fig. 2. It can be observed that at 1.65 kA the

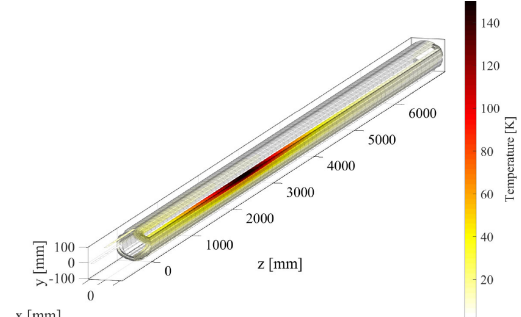


Fig. 3. Simulated 3D coil temperature profile at the end of the discharge following a quench at 2 kA without any quench protection.

baseline energy density is 10% to 55% higher than the minimum required to protect the magnet.

The CLIQ system is designed to protect the magnet above 6 kA even in the case no QH supplies were triggered. Designing CLIQ to assure protection at even lower currents is possible, but it would require a substantial increase of the unit capacitance. Since QH are fully redundant at low to medium current, as it will be shown shortly, such further improvement was not deemed necessary.

When the magnet is at low current (0–2 kA), the magnet is self-protected. This result is demonstrated with 3-dimensional electro-thermal simulations, where the thermal diffusion is modeled with the finite difference method [29]. The electrical resistance developed in the coil following a quench is sufficient to effectively discharge the transport current before T_{hot} rises excessively. It is shown that after a quench at 2 kA even in absence of quench protection the magnet current discharges in about 30 s. The simulated coil temperature profile at the end of the discharge is shown in Fig. 3. The peak coil temperature remains below 150 K.

At low to intermediate current (1–12 kA), the QH system, which is composed of eight independently-powered circuits, is fully redundant. The electrical and thermal transient following

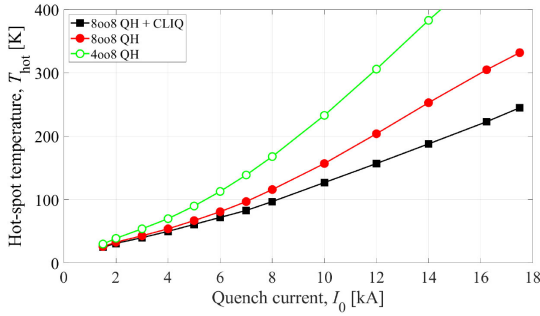


Fig. 4. Simulated coil adiabatic hot-spot temperature after a quench, versus initial magnet current. Baseline protection including eight QH units and CLIQ, and failure cases obtained with only QH, or with only half QH units.

TABLE I
MAIN MQXF MAGNET PARAMETERS [4], [7], AND [9]

Parameter	Unit	Value
Nominal current, I_{nom}	A	16230
Ultimate current, I_{ult}	A	17500
Peak field in the conductor at I_{nom}	T	11.3
Operating temperature	K	1.9
Differential inductance per unit length at I_{nom}	mH/m	8.2
Number of turns per pole	-	50

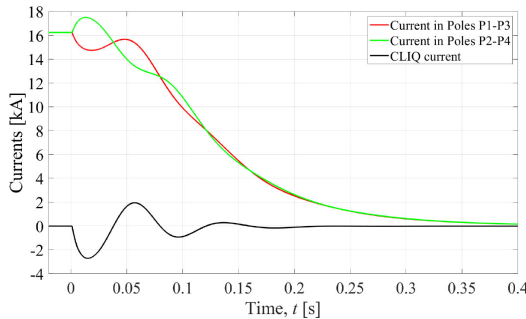


Fig. 5. Simulated currents in the 7.15 m magnet's coils sections, and introduced by the CLIQ unit, versus time, after a quench at nominal current.

a quench are simulated with the 2D quench program STEAM-LEDET for three cases: the baseline where eight out of eight QH supplies and the CLIQ unit are triggered (8008 QH + CLIQ), the failure case where only QH supplies are triggered (8008 QH), and the unrealistic failure case where only half of the QH supplies are triggered (4008 QH). The resulting hot-spot temperatures are shown in Fig. 4. For uniform conductor parameters, the simulated T_{hot} after a quench at 12 kA is about 160 K for the baseline case, about 210 K for the 8008 QH case, and about 310 K for the 4008 QH case. The probability of the latter case is negligible [30].

The quench protection of this magnet is most challenging at nominal and ultimate current (see Table I). The simulated currents in the magnet coils, and introduced by the CLIQ unit, after a quench in the 7.15 m magnet at the nominal current of 16.23 kA are shown in Fig. 5. The combined action of QH depositing heat through thermal diffusion and CLIQ depositing heat through inter-filament coupling loss transfers all coil turns to the normal state in less than 35 ms. As a result, the transport current is completely discharged in about 400 ms.

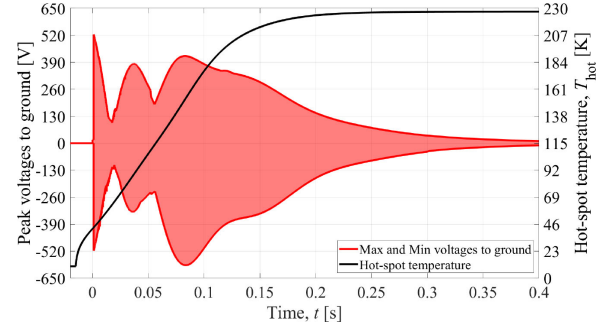


Fig. 6. Simulated coil adiabatic hot-spot temperature, and minimum and maximum voltages to ground, versus time, after a quench at nominal current.

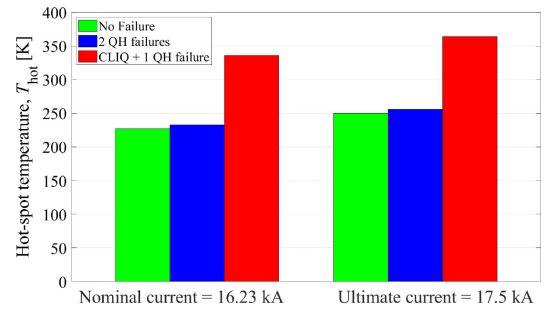


Fig. 7. Simulated adiabatic hot-spot temperature after a quench at nominal and ultimate current. Reference case in absence of failures, double QH unit failures, and CLIQ plus one QH unit failures.

The simulated T_{hot} , calculated conservatively under adiabatic conditions, reaches about 230 K (see Fig. 6). The minimum and maximum voltages to ground during the transient are also shown in Fig. 6. Immediately after triggering the protection system, the voltages are determined by the 1 kV voltage imposed by the CLIQ unit. The peak voltage to ground of 590 V, reached after about 90 ms, depends on the distribution of resistive and inductive voltages within the coils.

III. FAILURE CASES

The quench protection system is designed to assure protection in case of up to two simultaneous unit failures, i.e. either two QH units, or one QH unit and the CLIQ unit. The possibility that more than two independently powered and independently triggered units fail simultaneously is considered to be negligible. The impact of the failure of protection units on the protection performance is evaluated and summarized in Fig. 7, where the simulated T_{hot} at nominal and ultimate current are shown. In absence of failure, T_{hot} remains around 250 K even at the ultimate current of 17.5 kA. This temperature level is considered a very safe margin with respect to permanent coil degradation [31].

Simultaneous failure of two QH units would result in an increase of T_{hot} of less than 10 K. This result can be explained considering that at this high current level triggering CLIQ alone is sufficient to quickly transfer to the normal state most of the turns, and allows achieving a very fast current discharge.

Instead, simultaneous failure of one QH unit and of the CLIQ unit would result in a T_{hot} increase of almost 120 K at both current levels. The resulting temperature range of 340 to 370 K

TABLE II
RANGES OF THE MAIN CONDUCTOR PARAMETERS: AS DEFINED BY SPECIFICATIONS [32] AND AS EXPECTED FROM OBSERVATION

Parameter	Unit	Specification Range	Expected Range
Number of strands	-	40	40
Strand diameter	mm	0.85±0.003	0.85
Cu to non-Cu ratio	-	1.2±0.1	1.16-1.18
RRR ^a	-	≥100	200-250
Filament twist-pitch	mm	19±3	19
Strand twist-pitch	mm	109±3	109

^aRRR measured between 293 K and 20 K, after heat treatment.

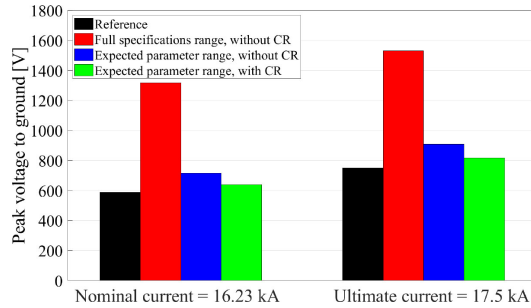


Fig. 8. Simulated peak voltages to ground after a quench at nominal and ultimate current. Reference case in absence of failures, and worst-cases obtained with most unfavourable conductor parameter distribution, or after coil reordering (CR).

is undesired, but considered acceptable for an extremely unlikely event such as a double failure.

Quench protection unit failures have also a significant impact on $U_{g,\text{peak}}$. In fact, different QH units heat up and induce a quench only in the coil turns to which they are glued, while CLIQ induces a quench more quickly in the two poles that receive a first positive current change, i.e. P2 and P4 (see Fig. 1). Given the presence of multiple inter-dependent effects, it is difficult to guess a priori the double-failure scenario that results in the highest $U_{g,\text{peak}}$. Thus, to identify the most critical cases dozens of combinations of QH and CLIQ failures are simulated. The findings are presented in the next section together with the conductor parameter analysis.

IV. CONDUCTOR PARAMETERS

The main conductor parameters are summarized in Table II, together with their ranges defined by specifications [32]. The two parameters that have the most significant effect on the $U_{g,\text{peak}}$ are the Cu to non-Cu ratio and the residual resistivity ratio (RRR), since they directly impact the conductor resistance. Thus, a non-uniform distribution of these two parameters among the four magnet coils would result in a non-uniform distribution of resistive voltages among them after a quench, and hence higher $U_{g,\text{peak}}$. The most unfavourable parameter distribution consists in two coils with lowest Cu to non-Cu ratio and lowest RRR in series to two coils with highest Cu to non-Cu ratio and highest RRR.

Quench transients in absence of failures and in presence of various types of double failures are simulated assuming the most unfavourable parameter distribution and the full ranges defined by specifications. The highest $U_{g,\text{peak}}$ obtained during these simulations, shown in Fig. 8, are about 1320 V and 1530 V at nominal and ultimate current, respectively. It should be noted

that these high figures, which are approximately twice higher than the reference case of 590 V (see Fig. 6), are obtained under excessively conservative assumptions.

The expected conductor parameter ranges, based on the delivered conductor, are significantly narrower than the specification ranges, as shown in Table II. Considering these realistic parameter ranges, the worst-cases $U_{g,\text{peak}}$ obtained for double failures and most unfavourable parameter distribution reach about 720 V and 910 V at nominal and ultimate current.

In order to further reduce $U_{g,\text{peak}}$ it is possible to optimize the electrical order of the four magnet coils, once an estimation of their real conductor parameters is available. Simulations show that reordering the four coils allows maintaining $U_{g,\text{peak}}$ at about 640 V and 820 V at nominal and ultimate current, which is less than 10% higher than the reference case, and compliant with the magnet's electrical design criteria [33].

V. CONCLUSION

The quench protection system of the High Luminosity LHC Inner Triplet circuit was described and analyzed with the STEAM-LEDET software. The circuit includes six Nb₃Sn quadrupole magnets powered in series, each individually protected by eight quench-heater units and one CLIQ unit. Upon quench detection all circuit protection elements are activated simultaneously.

It was shown that the designed system assures magnet protection over the entire operating current range. At currents below 2 kA, it was demonstrated by means of 3D simulations that the magnet is self-protected. At currents below 8 kA, while both quench-heater and CLIQ are activated, simulations show that even half of the QH units would be sufficient to maintain the coils hot-spot temperature well below 200 K. At nominal current in absence of equipment failures the baseline protection system maintains the hot-spot temperature below 230 K and the peak voltage to ground below 600 V.

The impact on the quench protection performance of simultaneous failures of two protection units, among the eight quench-heater and one CLIQ units, was assessed. The most critical case was found to be the simultaneous failures of the CLIQ unit and one quench-heater unit, which would result in an hot-spot temperature increase of 100 to 120 K at nominal and ultimate current. The obtained temperature range of 340 to 370 K is deemed acceptable for an extremely unlikely event such as a double failure.

Furthermore, it was shown that a non-uniform distribution in the four magnet coils of conductor parameters, and in particular the conductor Cu to non-Cu ratio and its RRR, can lead to large peak voltages to ground after a quench. Reducing the ranges of conductor parameters and selecting an optimum electrical order for the four magnet coils allows effectively reducing the worst-case voltage to ground, which can be maintained just 10% higher than the reference case.

ACKNOWLEDGMENT

The authors wish to thank B.Bordini (CERN) for his help in collecting MQXF superconductor parameters, and S. Yammine for the circuit schematic.

REFERENCES

- [1] G. Apollinari, O. Bröning, and L. Rossi, "High luminosity LHC project description," CERN, Geneva, Tech. Rep. CERN-ACC-2014-0321, Dec. 2014. [Online]. Available: <https://cds.cern.ch/record/1974419>
- [2] G. Apollinari, I. B. Alonso, O. Bröning, M. Lamont, and L. Rossi, "High-luminosity large hadron collider (HL-LHC): Preliminary design report," Geneva: CERN, 2015. [Online]. Available: <http://cds.cern.ch/record/2116337>
- [3] E. Todesco *et al.*, "A first baseline for the magnets in the high luminosity LHC insertion regions," *IEEE Trans. Appl. Supercond.*, vol. 24, no. 3, Jun. 2014, Art. no. 4003305.
- [4] P. Ferracina *et al.*, "Magnet design of the 150 mm aperture low- β quadrupoles for the high luminosity LHC," *IEEE Trans. Appl. Supercond.*, vol. 24, no. 3, Jun. 2014, Art. no. 4002306.
- [5] G. Ambrosio, "Nb₃Sn high field magnets for the high luminosity LHC upgrade project," *IEEE Trans. Appl. Supercond.*, vol. 25, no. 3, Jun. 2015, Art. no. 4002107.
- [6] E. Todesco *et al.*, "Design studies for the low-beta quadrupoles for the LHC luminosity upgrade," *IEEE Trans. Appl. Supercond.*, vol. 23, no. 3, Jun. 2013, Art. no. 4002405.
- [7] P. Ferracina *et al.*, "The HL-LHC low-beta quadrupole magnet MQXF: From short models to long prototypes," *IEEE Trans. Appl. Supercond.*, vol. 29, no. 5, Aug. 2019, Art. no. 4001309.
- [8] S. I. Bermudez *et al.*, "Progress in the development of the Nb₃Sn MQXFB quadrupole for the high luminosity upgrade of the LHC," *IEEE Trans. Appl. Supercond.*, 2020, submitted for publication.
- [9] E. Todesco, "Nominal and ultimate currents for WP3 HL-LHC IR magnets," CERN, Geneva, Tech. Rep. EDMS 2114564, v. 3.1, 2020.
- [10] E. Ravaoli, "Quench protection studies for the high-luminosity LHC inner triplet circuit," CERN, Geneva, Tech. Rep. EDMS 1760496, 2016.
- [11] E. Ravaoli *et al.*, "Advanced quench protection for the Nb₃Sn quadrupoles for the high luminosity LHC," *IEEE Trans. Appl. Supercond.*, vol. 26, no. 3, Apr. 2016, Art. no. 4002006.
- [12] E. Ravaoli *et al.*, "Quench protection system optimization for the high luminosity LHC Nb₃Sn quadrupoles," *IEEE Trans. Appl. Supercond.*, vol. 27, no. 4, Jun. 2017, Art. no. 4702107.
- [13] E. Todesco, "HL-LHC decision management: WP3 - Q1/Q2/Q3 protection baseline," CERN, Geneva, Tech. Rep. EDMS 1972818, 2018.
- [14] S. I. Bermudez *et al.*, "Overview of the quench heater performance for MQXF, the Nb₃Sn low- β quadrupole for the high luminosity LHC," *IEEE Trans. Appl. Supercond.*, vol. 28, no. 4, Jun. 2018, Art. no. 4008406.
- [15] E. Ravaoli *et al.*, "Quench protection performance measurements in the first MQXF magnet models," *IEEE Trans. Appl. Supercond.*, vol. 28, no. 3, Apr. 2018, Art. no. 4701606.
- [16] E. Ravaoli, "CLIQ," Ph.D. dissertation, Enschede, 2015, presented on Jun. 19, 2015. [Online]. Available: <http://doc.utwente.nl/96069/>
- [17] E. Ravaoli, V. I. Datskov, C. Giloux, G. Kirby, H. H. J. ten Kate, and A. P. Verweij, "New, coupling loss induced, quench protection system for superconducting accelerator magnets," *IEEE Trans. Appl. Supercond.*, vol. 24, no. 3, Jun. 2014, Art. no. 0500905.
- [18] V. Datskov, G. Kirby, and E. Ravaoli, "AC-current induced quench protection system," EU Patent EP13 174 323.9, Jun. 28, 2013, European Patent App. EP13174323.9, WO Patent App. PCT/EP2014/063575. [Online]. Available: <https://www.google.com/patents/WO2014207130A1?cl=en>
- [19] E. Ravaoli, B. Auchmann, M. Maciejewski, H. ten Kate, and A. Verweij, "Lumped-element dynamic electro-thermal model of a superconducting magnet," *Cryogenics*, 2016. [Online]. Available: <http://www.sciencedirect.com/science/article/pii/S0011227516300832>
- [20] "STEAM website," Feb. 9, 2021. [Online]. Available: <https://espace.cern.ch/steam/>
- [21] E. Ravaoli *et al.*, "Modeling of inter-filament coupling currents and their effect on magnet quench protection," *IEEE Trans. Appl. Supercond.*, vol. 27, no. 4, Jun. 2017, Art. no. 0500905.
- [22] M. Mentink and E. Ravaoli, "Analysis of MQXFS5 CLIQ tests of Nov. 2017," CERN, Geneva, Tech. Rep. EDMS 1930202, 2020.
- [23] E. Ravaoli *et al.*, "Quench protection of the first 4-m-long prototype of the HL-LHC Nb₃Sn quadrupole magnet," *IEEE Trans. Appl. Supercond.*, vol. 29, no. 5, Aug. 2019, Art. no. 4701405.
- [24] G. Chlachidze *et al.*, "Performance of the first short model 150-mm-aperture Nb₃Sn quadrupole MQXFS for the high-luminosity LHC upgrade," *IEEE Trans. Appl. Supercond.*, vol. 27, no. 4, Jun. 2017, Art. no. 4000205.
- [25] S. Stoynev *et al.*, "Summary of test results of MQXFS1—The first short model 150 mm aperture Nb₃Sn quadrupole for the high-luminosity lhc upgrade," *IEEE Trans. Appl. Supercond.*, vol. 28, no. 3, Apr. 2018, Art. no. 4001705.
- [26] J. F. Troitino, S. I. Bermudez, F. J. Mangiarotti, and S. F. Troitino, "Report on quench protection tests: MQXFS4c," CERN, Geneva, Tech. Rep. EDMS 2354774, 2020.
- [27] J. F. Troitino, S. I. Bermudez, M. Duda, and F. J. Mangiarotti, "Report on quench protection tests: MQXFS6," CERN, Geneva, Tech. Rep. EDMS 2354775, 2020.
- [28] M. Mangiarotti *et al.*, "Powering performance and endurance beyond design limits of HL-LHC low-beta quadrupole magnets models," *IEEE Trans. Appl. Supercond.*, 2020, submitted for publication.
- [29] E. Ravaoli, "Simulation of the 3D magnet quench process with the finite-difference method in STEAM-LEDET," CERN, Geneva, Tech. Rep. EDMS 2454468, 2020.
- [30] A. Apollonio, T. Cartier-Michaud, and A. Verweij, "Reliability studies for HL-LHC inner triplet magnets protection," CERN, Geneva, Tech. Rep. EDMS 2308131, 2019.
- [31] G. Ambrosio, "Maximum allowable temperature during quench in Nb₃Sn accelerator magnets," in *Proceedings, WAMSDO 2013 Workshop on Accelerator Magnet, Superconductor, Design and Optimization: CERN Geneva, Switzerland, 15-16 Jan. 2013*, no. FERMILAB-CONF-13-593-TD, 2013, pp. 43–46. [Online]. Available: <https://inspirehep.net/record/1277941/files/arXiv:1401.3955.pdf>
- [32] L. D. Cooley, A. K. Ghosh, D. R. Dietderich, and I. Pong, "Conductor specification and validation for high-luminosity LHC quadrupole magnets," *IEEE Trans. Appl. Supercond.*, vol. 27, no. 4, Jun. 2017, Art. no. 6000505.
- [33] T. da Rosa and F. R. Mateos, "Electrical design criteria for the HL-LHC inner triplet magnets," CERN, Geneva, Tech. Rep. EDMS 1963398, 2020.